

Supplementary material: Is the methanation reaction over Ru single crystals structure dependent?

Søren B. Vendelbo, Martin Johansson, Jane H. Nielsen, and Ib Chorkendorff

Center for Individual Nanoparticle Functionality (CINF),

Department of Physics, Building 312,

Technical University of Denmark, 2800 Kgs. Lyngby, Denmark

In order to describe the conditions inside the HPC, two approaches are taken: One approach is based on Computational Fluid Dynamics (CFD) to simulate both global and local signals. In the other approach, the equations describing a simplified local system are solved analytically. Below, both approaches are documented.

CFD model of the HPC – global and local signals

In order to model the flow, temperature, and gas concentrations inside the HPC, a CFD simulation using the finite element method implemented in COMSOL Multiphysics was performed. The model assumes axial symmetry with the capillary center as the symmetry axis. The material dependent parameters such as viscosity and heat conductivity were taken from the Comsol materials library and ref. [1]. The flow profile obtained from the simulations was compared to an analytical solution taking advantage of the cylindrical geometry, and good agreement was obtained. It was found that the flows of heat and

mass in and out of the HPC were equal within computational errors. The model takes both heat conduction and convection into account. The density, dynamic viscosity, thermal conductivity, and heat capacity of the gas inside the HPC are assumed to have the corresponding values for hydrogen. The pressure change due to chemical changes of the gas is not taken into account. These assumptions are reasonable for our HPC because we always have a large surplus of hydrogen (99 %), resulting in a decoupling of the concentration from the flow and temperature, and resulting in a reduction of the computational complexity of the problem.

The simulated gas flow inside the HPC is depicted in Figure S1a. The arrows indicate the direction of the flow and the color indicates the velocity measured in m/s. The line in the middle is the symmetry axis. Convection due to the temperature of the crystal is seen. Figure S1b shows an enlargement of the crystal and the nozzle. Notice the large gas velocity under the aluminum nozzle and the small velocity below the capillary. Any small changes of the nozzle and capillary position change the flow profile and since the back diffusion is exponentially damped by this flow, small changes in these positions will severely change the measurement. Hence all experiments in the HPC are carried out with the nozzle at the same distance from the sample with a small uncertainty (0.30 ± 0.01 mm).

In Figure S2a, the temperature distribution inside the HPC is shown. The middle of the crystal is set to 700 K and the walls of the HPC are set to 300 K. In reality the walls will heat up over time to approximately 320 K but during the time of one methanation experiment a wall temperature of 300 K is a reasonable assumption. When the aluminum nozzle is close to the sample it removes heat from the sample. This is seen in Figure S2b

where the aluminum nozzle has a temperature between 500 K and 550 K. Even though the nozzle is less than one millimeter away from the sample, the temperature of the sample is very uniform. The temperature difference within the sample is less than 5 K as illustrated in Figure S2c.

Using the model for the gas flow described above, the concentration of methane can be simulated inside the HPC. If a full microkinetic description should be given, the methane production rate from the catalytic active surface should depend on both the CO and hydrogen pressures. Normally the high CO pressures would cause site blocking due to the relative high bonding energy of CO and that would naturally vary over the entire crystal as a function of the local CO pressure. Similarly, it is also known that the reaction is half order in hydrogen due to the COH dissociation being the rate limiting step (ref [9] in Paper). Here, however, the aim is not to obtain a complete quantitative model and since furthermore the CO pressure is very low (10 mbar) as compared to hydrogen (1000 mbar) these effects are expected to be negligible. Therefore the methane production is merely simulated at any point on the ruthenium crystal surface as a function of the local CO pressure. In order to do so, we assume a very simple model for the methane formation rate:

$$r_{CH_4} = k_0 \theta_{CO} = k_0 \frac{p_{CO}^0 - p_{CH_4}}{\sqrt{2\pi m k_B T}} \quad (3)$$

Here, r_{CH_4} is the rate of methane formation per area, k_0 is a constant, and θ_{CO} is the flux of CO molecules impinging on the surface which can be expressed by the initial CO pressure, p_{CO}^0 , minus the methane pressure, p_{CH_4} . The molecular mass of CO is described by m , the Boltzmann constant by k_B , and the gas temperature by T . Ideal gas behavior is

assumed in all calculations. In this model, k_0 acts as an overall reaction probability, where all the details of the intermediate reaction steps such as dissociation, recombination, and desorption are collected.

Based on our simplified model, we can compute the concentration and thus the mole fraction of methane within the reactor volume as a function of the overall reaction probability, k_0 . In order to model the experimentally determined global and local measurements, the methane mole fraction, χ_{CH_4} , divided by the initial CO mole fraction, $\chi_{CO-start}$, is computed at the HPC reactor outlet (corresponding to the global measurement) and right above the single crystal surface in the flow of the inlet gas however in a stagnant gas layer (corresponding to the local measurement). The ratio, $\chi_{CH_4} / \chi_{CO-start}$, for the global and local situations is shown as a function of k_0 in Figure S3. The positions of the calculations are indicated by black circles in the inserts. Both the global and local methane mole fractions increase linearly with k_0 initially and levels off at higher k_0 values when approaching full conversion. Notice that the thermodynamics is in favor of full conversion at temperatures below 700 K.

In order to find the corresponding turnover frequency (TOF) values as a function of k_0 , we will start by expressing the local TOF as the methane production rate described in equation (3) divided by the number of active sites per area, N_s :

$$TOF_{CH_4,local} = \frac{r_{CH_4}}{N_s} \quad (4)$$

This is proportional to the local concentration of methane and will vary with the position in the HPC as illustrated by the inserts in Figure S3. TOF values averaged over the entire

HPC called $TOF_{CH_4,global-avg}$ can be found for a given k_0 based on the simulated values for the methane mole fraction, χ_{CH_4} and the flow:

$$TOF_{CH_4,global-avg} = \frac{\chi_{CH_4}}{AN_s} F \quad (5)$$

where A is the active area (sum of the front-side, sides, and backside) and F is the flow of gas at the outlet of the HPC expressed in number of molecules per second. The calculated $TOF_{CH_4,global-avg}$ values are shown as the right axis in Figure S3. The TOF at initial conditions where no CO has been consumed yet is also computed. This is denoted $TOF_{CH_4,max}$ and is shown on the top horizontal axis in Figure S3. As expected, $TOF_{CH_4,max}$ is directly proportional to k_0 which is the pure reaction probability without considerations of the influence of the availability of reactant gas. At low k_0 values, the average and maximum TOF values are the same because a negligible amount of CO is consumed. At k_0 values above 10^{-5} or TOF values above $\sim 10 \text{ s}^{-1}$, the average and maximum TOF values diverges. For TOF values between 0.1 and 10 s^{-1} , the local methane pressure will thus be proportional to the local reaction rate. At TOF values lower than this, the methane concentrations are too low to be measured by the QMS, and TOF values higher than 10 s^{-1} result in mass transport limitations for the specific gas composition used here. The difference between the global and local methane signals is approximately a factor of ten, so the local measurement should not be completely diluted by the inlet gas but is certainly still a challenge to measure.

In a computational environment, it is possible to "switch off" the front-side reactivity and study the effect on the global and local signals. The results are shown as dashed lines in Figure S3. The global signal (blue dashed line) decreases as expected compared to the original global signal (blue line) with an amount corresponding to the decrease in active

surface area (~30 %). The effect on the local signal, however, is much stronger and a reduction of four orders of magnitude is observed. The small signal remaining is from back diffusion from the surroundings, so ideally the influence from the backside and sides of the single crystal on the local measurement should be negligible in our experimental setup.

In reality, however, experiments where CH₄ is let into the HPC through a separate entry while pure H₂ flows through the nozzle, reveals a local signal which is at least two orders of magnitude higher than predicted by the model. This can either be due to an incorrect description of the transport rate between the gas surrounding the sample and the capillary, most likely caused by a slight misalignment between nozzle and sample, or be due to a leak between the aluminum nozzle and the gas inlet tube.

In order to correct for the contribution to the local methane signal from the partial pressure in the rest of the HPC, Ar is let into the HPC through a separate entry, at the same time as CO and hydrogen are introduced through the nozzle. The ratio between the partial pressure of Ar measured locally and globally is a measure of the transport rate from the volume surrounding the sample towards the capillary.

It is assumed that the gas composition in the volume surrounding the sample is homogeneous, and that the concentrations of Ar and CH₄ are small, so that the problem is one of diffusion of these gases in hydrogen. Since the concentration of CH₄ is small, it is furthermore assumed that the local production rate of CH₄ is independent of the local partial pressure of CH₄. Under these conditions the local partial pressure of CH₄ is described by a linear partial differential equation. The total partial pressure of CH₄ at the capillary, $p^{local}_{CH_4}$, can be expressed as the sum of the contributions from the production

of the front of the crystal, $p^{local,front}_{CH_4}$ and the contribution from the rest of the crystal, $p^{local,rest}_{CH_4}$. The same reasoning applies to the global partial pressure of CH_4 , so that $p^{global}_{CH_4} = p^{local,front}_{CH_4} + p^{local,rest}_{CH_4}$. From measurements where Ar and CH_4 are let into the HPC while hydrogen flows through the nozzle, we know that p^{local} is proportional to p^{global} . Hence

$$p^{local,rest}_{CH_4} = B p^{global,rest}_{CH_4} \frac{P_{Ar}^{local}}{P_{Ar}^{global}} \quad (6)$$

where B is a proportionality factor due to the use of two different QMS's. From this we find that

$$P_{CH_4}^{local,front} = P_{CH_4}^{local} - B p^{global,rest}_{CH_4} \frac{P_{Ar}^{local}}{P_{Ar}^{global}} \quad (7)$$

Since any difference in the transport rate between CH_4 and Ar is due to differences in the diffusivities, which are equal to within 10 % in the temperature range 300 - 700 K [2] it can safely be assumed that B is constant. Since $p^{local,front}_{CH_4} \ll p^{local,rest}_{CH_4}$, see Figure 4 in Paper, it is a reasonable approximation to set

$$P_{CH_4}^{local,front} = P_{CH_4}^{local} - B p^{global}_{CH_4} \frac{P_{Ar}^{local}}{P_{Ar}^{global}} \quad (8)$$

The global contribution to the local signal described by the latter term contributes with 30 - 80 %, depending on the sulfur coverage. This false contribution can, however, be accounted for and subtracted in each experiment, so that a truly local signal is obtained.

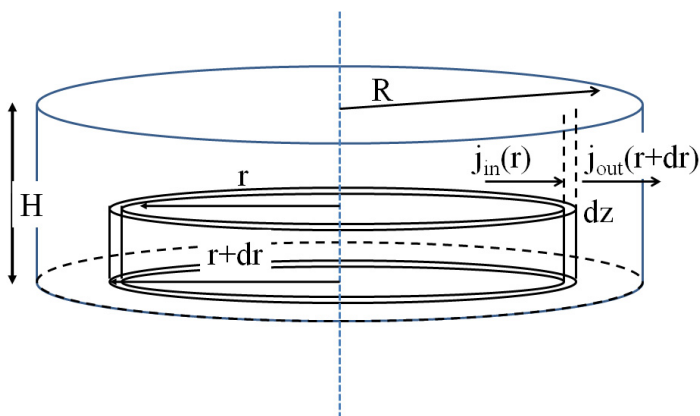
Simple model of the HPC – estimate of the local signal

In order to gain insight into the design parameters that are most important for measuring the local signal, a simple analytical model can be established. In the following we shall consider the volume in between the crystal surface and the sniffer as a cylinder with radius R (1 mm) and height H (0.3 mm). The diffusion constant D is typically $1.65 \text{ cm}^2/\text{s}$ at 500 K for methane in Hydrogen (equimolar) meaning that the diffusion is fast when compared to the dimension of R and H . Thus instead of considering the molecules being generated at the surface of the crystal at the bottom of the cylinder at a rate per area ($\text{m}^{-2}\text{s}^{-1}$), r_{CH_4} , we can safely assume they are generated homogeneously over the entire volume. This latter term is denoted R_{CH_4} . The rates can be expressed in terms of density of sites on the surface and TOF of these sites as:

$$r_{CH_4} = TOF \cdot N_s \qquad R_{CH_4} = \frac{r_{CH_4}}{H} = \frac{TOF \cdot N_s}{H} \quad k_0 = TOF \cdot N_0$$

$$k_0 = \frac{r_0}{H} = \frac{TOF \cdot N_0}{H} \qquad (1)$$

Notice the dimension of R_{CH_4} is concentration per second ($\text{m}^{-3}\text{s}^{-1}$) and N_s is the number of active sites per area.



We are now considering the number of molecules per time, J , moving in and out of the volume between two concentric cylinders both with height H and radii r and $r+dr$. Since we are studying equilibrium we know that what has gone out equals what has gone in plus what has been generated in that volume element, so

$$J_{out}(r+dr) = J_{in}(r) + R_{CH_4} \cdot 2\pi \cdot H \cdot r \cdot dr \quad (2)$$

$$2\pi \cdot H \cdot (r+dr) \cdot j_{out}(r+dr) = 2\pi \cdot H \cdot r \cdot j_{in}(r) + R_{CH_4} \cdot 2\pi \cdot H \cdot r \cdot dr \quad (3)$$

We eliminate j by using Fick's 1st law which relates the flux, j , to the diffusion constant,

$$D, \text{ and the concentration, } C: j = -D \frac{dC(r)}{dr} \quad j = -D \frac{dC(r)}{dr}$$

$$(r+dr) \cdot D \cdot \frac{dC(r+dr)}{dr} = r \cdot D \cdot \frac{dC(r)}{dr} - R_{CH_4} \cdot r \cdot dr \quad (4)$$

which can be rewritten into

$$(r+dr) \frac{dC(r+dr)}{dr} - r \frac{dC(r)}{dr} = -\frac{R_{CH_4} \cdot r \cdot dr}{D} = -\frac{r_{CH_4} \cdot r \cdot dr}{H \cdot D} \quad (5)$$

By neglecting higher order terms and using this identity

$$\frac{dC(r)}{dr} = \frac{C(r+dr) - C(r)}{dr} \Rightarrow C(r+dr) = dr \cdot \frac{dC(r)}{dr} + C(r) \quad (6)$$

We obtain the following differential equation

$$\frac{d^2C(r)}{dr^2} + \frac{1}{r} \frac{dC(r)}{dr} = \frac{1}{r} \frac{d}{dr} \left(r \frac{dC(r)}{dr} \right) = -\frac{r_{CH_4}}{H \cdot D} \quad (7)$$

This can be solved by simple integration leading to:

$$C(r) = -\frac{r_{CH_4}}{4H \cdot D} r^2 + b \ln r + c \quad (8)$$

where b and c are integration constants. By assuming that the reactant gas is efficiently sweeping away any products outside the cylinder, we get the constraint $C(r)=0$ for $r=R$.

Similarly for symmetry reasons: $\frac{dC(r)}{dr} = 0$, for $r=0$ leading to

$$C(r) = \frac{r_{CH_4}}{4H \cdot D} (R^2 - r^2) \quad (9)$$

Thus the maximum concentration is at $r = 0$, which is the point where we are probing the local concentration:

$$C_{MAX} = C(r = 0) = \frac{r_{CH_4} \cdot R^2}{4H \cdot D} \quad (10)$$

This formula can be used to determine the concentration of methane just below the sniffer at $TOF=1 \text{ s}^{-1}$ as:

$$C_{MAX} = \frac{1.58 \cdot 10^{19} \frac{1}{\text{s} \cdot \text{m}^2} \cdot (1 \cdot 10^{-8} \text{ m})^2}{4 \cdot 3 \cdot 10^{-4} \text{ m} \cdot 1.65 \cdot 10^{-4} \text{ m}} = 8.0 \cdot 10^{19} \text{ m}^{-3} \quad (12)$$

In the experiments performed here the methane concentration is measured relative to the inlet CO concentration (10 mbar) at $T = 500 \text{ K}$

$$C_{CO}^{inlet} = \frac{P_{CO}}{k_B T} = \frac{0.01 \cdot 10^5 \text{ Pa}}{1.38 \cdot 10^{-23} \text{ J/K} \cdot 500 \text{ K}} = 1.44 \cdot 10^{23} \text{ m}^{-3} \quad (13)$$

Thus the predicted local methane concentration relative to the initial CO concentration is $5.5 \cdot 10^{-4}$. The simulations presented in Figure S3 gives a fraction of $1 \cdot 10^{-3}$ for $TOF = 1 \text{ s}^{-1}$ which is in reasonable agreement, considering that the approximation of zero concentration outside the cylinder is idealized. It is worth noticing that optimal signal is obtained for a close proximity to the crystal and that is scales with the square of the radius of the gas cylinder.

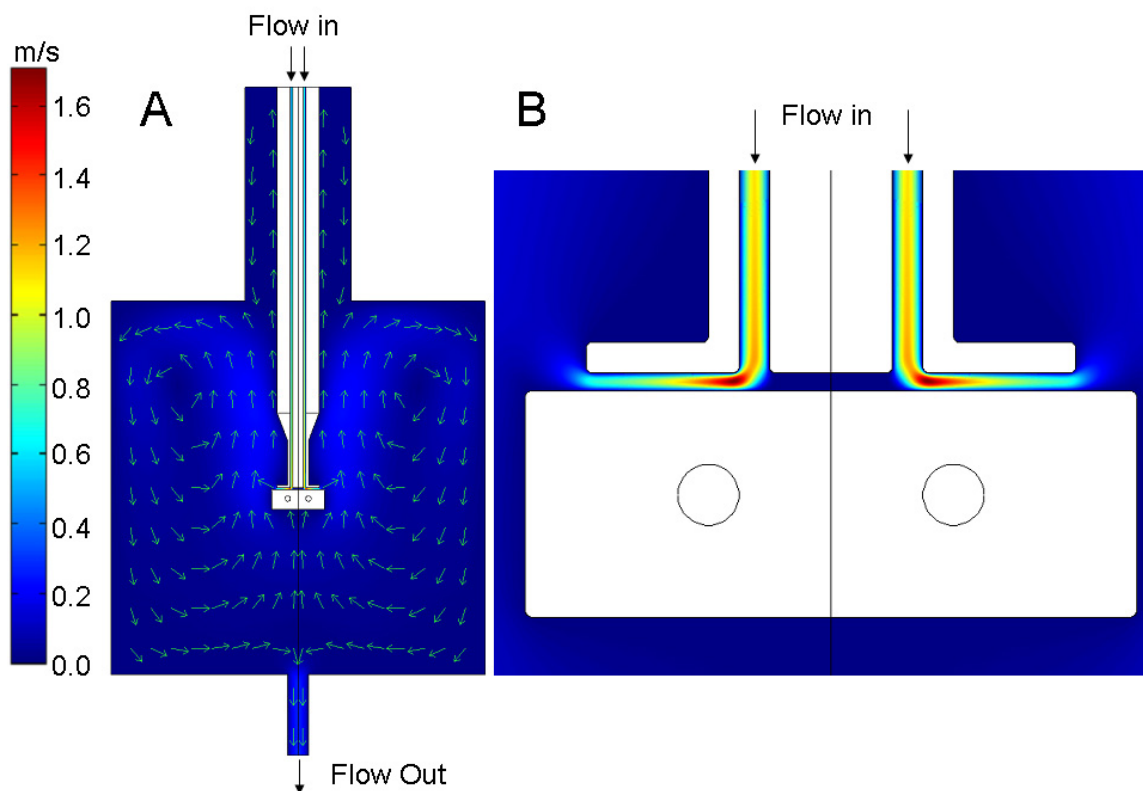


Figure S1. The simulated flow inside the HPC (A). The arrows indicate the direction and the color corresponds to the gas velocity. An enlargement of the flow profile around the nozzle and the sample is shown in (B). The color scale shown to the left is the same for images in (A) and (B). The largest gas velocity is seen to be between the sample and the nozzle, but the velocity below the capillary is close to zero. The line down the middle is the symmetry axis.

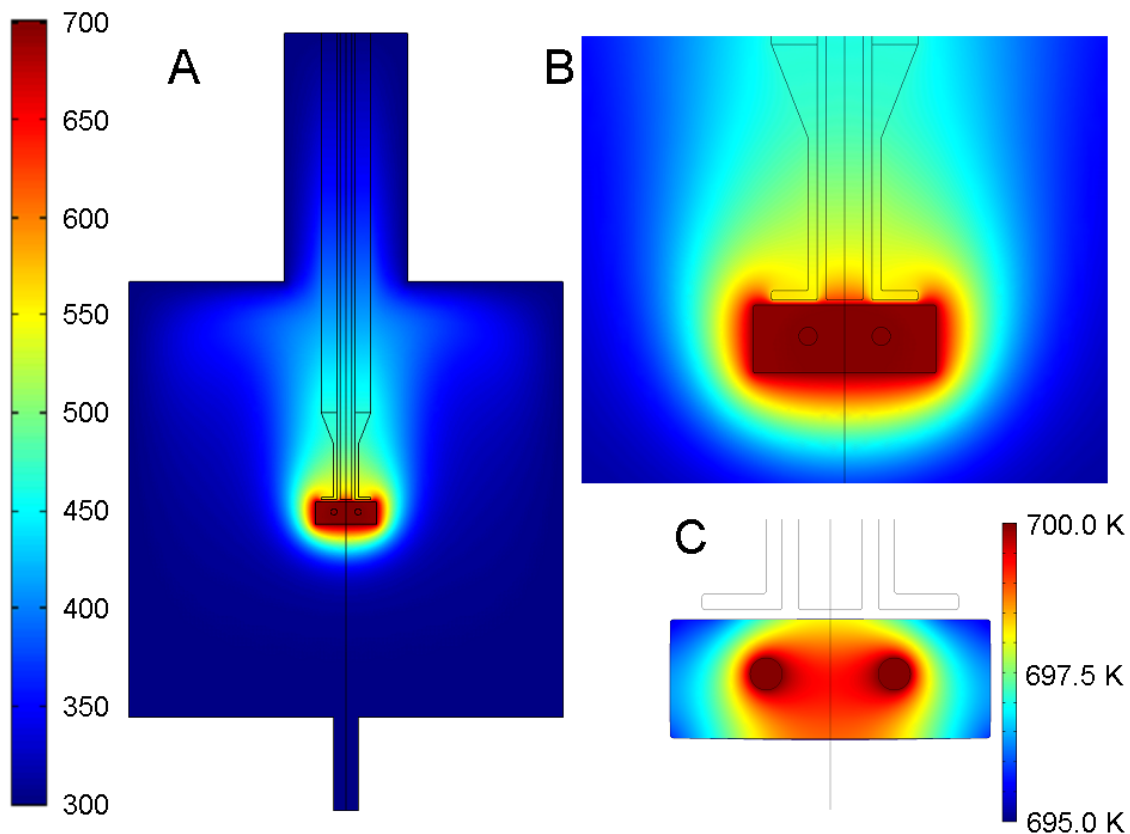


Figure S2. The temperature distribution inside the HPC with the sample at 700 K and the walls of the HPC at 300 K is shown in (A). An enlargement of the nozzle and sample is shown in (B). The colorscale for (A) and (B) is shown to the left. It is seen that the nozzle is heated by the sample at 700 K, and hence removes energy from the crystal front. The temperature distribution of the crystal only varies 5 K over the entire crystal, being 695 K at the edges and 700 K at the position of the heating wires, see (C) with separate colorscale shown to the right.

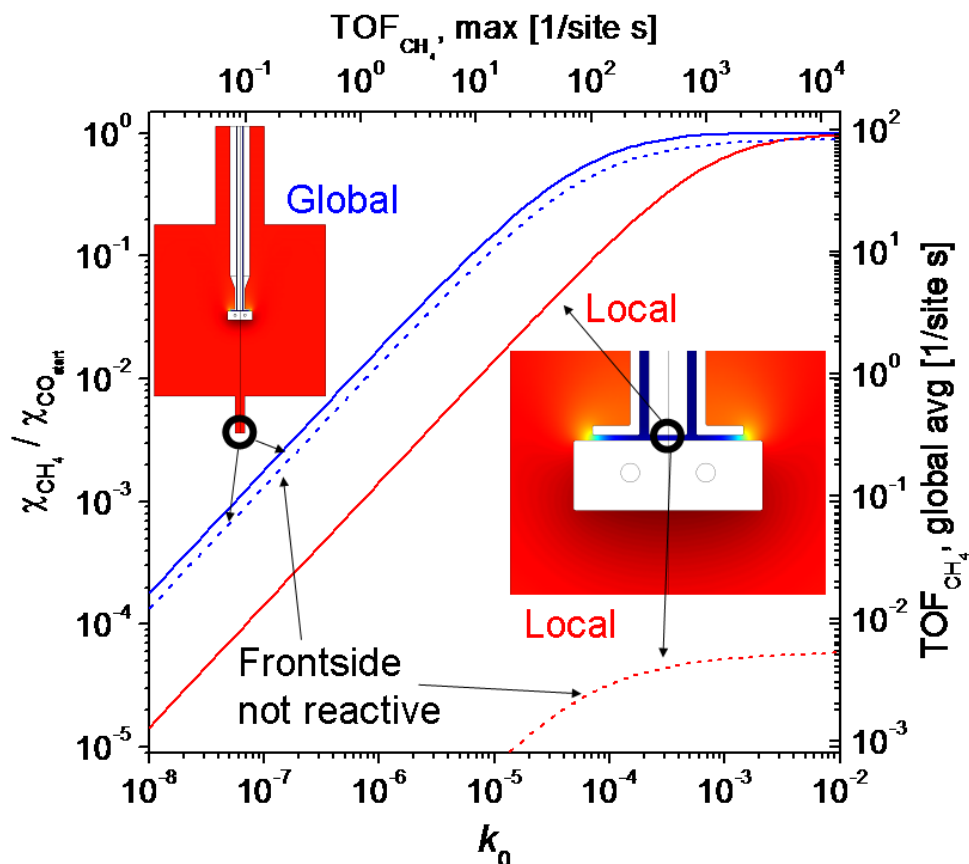


Figure S3. The simulated mole fraction of methane divided with the inlet mole fraction of CO as a function of k_0 . The temperature is 500 K. The blue and red lines are the calculated methane signal corresponding to the global and local measurements, respectively. The dashed lines are simulations with the front-side reactivity set to zero. The insets show the methane distribution, and the black circles show where the global and local signals are calculated. The calculation of the corresponding TOF values is explained in the text.

References

[1] David R. Lide, editor. *Handbook of Chemistry and Physics*, 89th Edition (Internet Version 2009) . CRC Press/Taylor and Francis, Boca Raton, FL., 2009.

[2] R.B. Bird, W.E. Stewart, and E.N Lightfoot. *Transport Phenomena* (Second Edition ed.) . John Wiley & Sons, 2001.